TR (BR)-10/96-97

EFFECT OF CHANNEL CHARACTERISTICS ON FLOOD WAVE PROPAGATION

NATIONAL INSTITUTE OF HYDROLOGY
JAL VIGYAN BHAWAN
ROORKEE - 247 667

CONTENTS

	Page No.
List of Figures	(i)
List of Tables	(ii)
ABSTRACT	(iii)
INTRODUCTION	1
NWS DAMBRK MODEL	4
EFFECT OF CHANNEL CHARACTERISTICS	6
ANALYTICAL DERIVATIONS	19
CONCLUSION	26
REFERENCES	27

LIST OF FIGURES

No.	Title	Page No.
1	Vaigai dam break flood hydrograph.	7
2	Vaigai dam failure study.	8
3	Dimensionless hysteresis Vs. attenuation per km.	9
4	Dimensionless hysteresis Vs. phase difference.	10
5	Assumed channel characteristics for various test runs.	12
6	Impacts of channel shape,contraction,expansion-contraction combination, and contraction-expansion combination.	14
7	Figure showing impacts of bed slope (So), Manning's roughness (n), flood plain (FP1 & FP2), and inactive storage (Ao).	17
8	Comparison of computed non-dimensional hystereses (Eq. 1) and those derived analytically (Eq. 9); data (*) & (**) used by Mishra and Seth(1996); and (***) by Mishra et. al (1977).	21
9	Relation between non-dimensional hysteresis and logarithmic decrement (dimensionless). Data (*) & (**) used by Mishra and Seth(1996); and (***) by Mishra et. al (1977).	22
10	Observed loop rating curves (dimensionless)	23

LIST OF TABLES

No.	Title	Page No.
1	Criteria for wave types	2
2	Description of test runs	11
3	Summary of computed hysteresis (η) for the test runs	11
4	Characteristics of input flood waves	20
5	Details of the flood events observed on the rivers in Gujarat (India)	25
6	Application results of observed flood events	25

ABSTRACT

Describing flood wave propagation in open channel flow with in the frame-work of loop or hysteresis of rating curves has not received much attention though frequent attempts have been made time and again. The presented description in literature has been more intuitive than being rational. The available know-how restricts to that (i) the hysteresis is a manifestation of channel storage and is a phenomenon; (ii) the channel roughness causes unsteadiness in the flow and gives rise to the development of hysteresis in the rating curve at a site; and (iii) the larger hysteresis pertains to the larger flood wave attenuation and vice versa. The shifting control situations also causes hysteresis in the rating curves and it, however, is beyond the scope of the present report.

The present work is an attempt to describe the flood wave propagation in natural and artificial channels within the perspective of site-specific rating curve. This work is a further extension of the earlier works carried out at the institute. In steps, the study on looking at the impacts of channel characteristics-- bed slope, flood plains, channel shape, expansion-contraction combination, expansion-contraction combination, inactive storage, Manning's roughness, expansion, and contraction-- on flood wave propagation deals with:

1) the dam break flood computation for Vaigai dam and routing through the downstream channel using National Weather Service's Dam Break Flood Forecasting (NWS DAMBRK) Model;
2) the development of the dimensionless rating curves at all the downstream cross-sections and then computation of hysteresis (η);
3) the analysis of the dam break flood wave propagation characteristics using η-values; and
4) the analysis for the impacts of above channel characteristics on the above dam break flood wave propagation in a hypothetical channel of approximately the same length as of above downstream river reach of Vaigai dam.

Further, the analytically derived relationship between quantified hysteresis (η) and phase difference (ϕ) is verified using the available numerically derived and observed data. Also, for kinematic wave situation, a unique relationship among η, ϕ, and logarithmic decrement δ is presented.

INTRODUCTION

Hysteresis represents loop in a rating curve. It has intuitively been used to describe the attenuation characteristics of flood waves since long. Hysteresis (η) is defined as the area of the loop in a non-dimensional rating curve (Mishra and Seth, 1994, 1996; Mishra et al.,1997; Jain et al.,1996; Mishra et al., 1996). It can be expressed mathematically as below:

$$\eta = \frac{1}{2}\int_0^T \left(q\frac{dh}{dt} - h\frac{dq}{dt} \right) dt \qquad (1)$$

where,

$$h = \frac{H - H_{min}}{H_{max} - H_{min}}; \text{ and} \qquad (2)$$

$$q = \frac{Q - Q_{min}}{Q_{max} - Q_{min}} \qquad (3)$$

Here, T is the time period of the flood wave (= time of rise and time of recession); h is the dimensionless stage (a function of time, t); H_{max} is the maximum computed depth at a site of interest; H_{min} is the minimum computed depth at a site of interest; and H is the computed depth (time varying function) at a site of interest. Similarly, Q and q stand for discharge and dimensionless discharge, respectively. Taking the analogy of Hagen's dam factor, Mishra and Seth(1996) and others described hysteresis as an index of energy expended by the flood wave during its time period.

The attempts on describing the flood wave characteristics within the frame-work of loop rating curve, in particular, commenced after Henderson(1966). The later works of Cunge et al. (1980), French(1985) and Ponce(1989) are worth citing. Mishra and Seth(1994, 1996) described the flood wave characteristics, viz. wave celerity, phase difference (ϕ) and attenuation, using the above described hysteresis, η (postulated range 0-1), and developed hysteresis criteria for defining wave kinds e.g. kinematic, diffusion and dynamic waves (Table 1). In Table 1, F_o is the Froude number. The results of their study were further supported and verified by Jain et al.(1996) and Mishra et al.(1997)

who also gave a definite relationship between η and ϕ. Following these works, Mishra et al. (1996) extended their study to see the impacts of channel characteristics, shape and expansion/contraction, on flood wave propagation and applied above η-ϕ relationship to the field data. The envisioned applications(Mishra et al. ,1997) of such a study are: (i)to identify wave kinds in natural channels for applying suitable simplified routing model;(ii)to locate fictitious downstream boundary for improving National Weather Service's Dam Break Flood Forecasting Model's(NWS DAMBRK) results;(iii)to compute time base of the flood hydrograph; and (iv) to process the discharge hydrographs derived using engineer's rating curve for phase difference.

TABLE 1. CRITERIA FOR WAVE TYPES

Wave type	Hysteresis (η) (dimensionless)	Wave number, $\hat{\sigma}$, and $\hat{\sigma}F_o$ (dimensionless)	Phase difference (ϕ) (radians)
Kinematic	$\eta < 0.025$	$\hat{\sigma} \leq 0.03$	$\phi < 0.03$
Diffusion	$0.025 \leq \eta \leq 0.10$	$\hat{\sigma}F_o \leq 0.462$	$0.03 \leq \phi \leq 0.13$
Dynamic	$\phi > 0.10$	$\hat{\sigma}F_o > 0.462$	$\phi > 0.13$

Source: Mishra and Seth(1994,1996)

Menendez and Norscini(1982) described the attenuation characteristics in terms of phase difference, ϕ, for which a mathematical form for computation purpose was given by Mishra and Seth(1994,1996) as below:

$$\phi = \frac{2\pi}{T}(t_{ph} - t_{pQ}) \tag{4}$$

where, ϕ is in radian; T is in hr; t_{ph} is the time of rise of stage wave (hr); and t_{pQ} is the time of rise of discharge wave (hr). Menendez and Norscini(1983) described ϕ as a kinematic parameter that drives attenuation. Ponce and Simons(1977) described wave attenuation using logarithmic decrement, δ, which was later shown to be related with the ϕ (Menendez and Norscini, 1983). Mishra et al.(1997) gave the following equation for computing δ:

$$\delta = \frac{cT}{\Delta x}(\ln Q_j - \ln Q_{j-1}) \quad (5)$$

where, δ is the logarithmic decrement in one period of wave travel (dimensionless); T is in seconds; Q_{j-1} and Q_j are the peak discharges (cumec) at successive locations j-1 and j, respectively; and Δx is the reach length in m; c is the wave celerity ($=\Delta x/tt$) (m/s); and tt is the time of travel (second). Greater δ corresponds to greater attenuation and vice versa.

In the present report, the impacts of channel characteristics, viz. bed slope, Manning's roughness, channel shape, expansion, contraction, contraction-expansion combination, expansion-contraction combination, and flood plain on flood wave propagation have been studied using the quantified hysteresis of site-specific rating curve.

NWS DAMBRK MODEL

The National Weather Service's Dam Break Flood Forecasting (NWS DAMBRK) model used in this study is described in brief. It is a combination of dam breach and flood routing mechanisms. Both are described below:

Breach Mechanism

The breach is the opening formed in the dam as it fails. The actual failure mechanics is not well understood for either earthen or concrete dams. Earthen dams which exceedingly outnumber all other types of dams do not tend to completely fail, nor do they fail instantaneously. The fully formed breach in earthen dams tends to have an average width (b) in the range ($h_d < b < 3h_d$) where h_d is the height of the dam. The breach widths are, therefore, much less than the total length of the dam as measured across the valley. Also, the breach requires a finite interval of time for its formation through erosion of the dam materials by the escaping water. Total time of failure may be in the range of a few minutes to a few hours, depending on the height of the dam, the type of materials, the extent of compaction of the materials used in construction, and the extent (magnitude and duration) of the overtopping flow of the escaping water. Piping failures occur when initial breach formation takes place at some point below the top of the dam due to erosion of an internal channel through the dam by escaping water. As the erosion proceeds, a larger and larger opening is formed; this eventually hastened by caving-in of the top portion of the dam. Concrete gravity dams also tend to have a partial breach as one or monolith sections formed during the construction of the dam are forced apart by the escaping water. The time for breach formation is in the range of a few minutes. Poorly constructed earthen dams and coal-waste slag piles which impound water tend to fail within a few minutes, and have average breach widths in the upper range or even greater than those for the earthen dams mentioned above.

The shape is specified by a parameter z identifying the side slope of the breach, i.e., 1 vertical : z horizontal slope. The range of z values is : $0 \leq z \leq 2$. Rectangular, triangular, or trapezoidal shapes may be specified in this way. The final breach size is controlled by the z parameter and another parameter, the terminal width of the bottom of the breach. The model assumes the model breach width starts at a point and enlarges

at a linear rate over the failure time interval until the terminal breach width is attained and the breach bottom has eroded to the elevation which is usually, but not necessarily, the bottom of the reservoir or outlet channel bottom. If the time of failure is less than 10 minutes, the width of the breach bottom starts at a value of final breach width rather than at a point. This represents more of a collapse failure than an erosion failure.

Flood Routing

The above described breach mechanism is coupled with the reservoir routing to compute the dam break flood hydrograph which is routed to the downstream end of the channel. The reservoir routing is carried out either by Modified-Puls method or by dynamic routing, depending on the level of accuracy desired. The modified Puls method requires reservoir characteristics, viz. elevation-capacity or -surface area table and the inflow, to the reservoir, hydrograph ordinates. The dynamic routing, however, requires complete details of channel characteristics, viz. elevation-top width table, Manning's roughness, channel expansion/contraction coefficients, cross-section location etc. The dynamic routing both in reservoir and channel is carried out using the numerical solution (four-point finite difference implicit scheme) of the following St. Venant's equations:

$$\frac{\partial Q}{\partial x} + \frac{\partial (A+A_o)}{\partial t} - q = 0 \qquad (5a)$$

$$\frac{\partial Q}{\partial x} + \frac{\partial (\frac{Q^2}{A})}{\partial x} + gA(\frac{\partial h}{\partial x} + S_f + S_e) = 0 \qquad (5b)$$

where, A is the active cross-sectional area of flow, A_o is the inactive (off-channel storage) cross-sectional area, x is the longitudinal distance along the channel (valley), t is the time, q is the lateral inflow or outflow per linear distance along the channel (inflow is positive and outflow is negative in sign), g is the gravitational acceleration due to gravity, S_f is the friction slope, S_e is the expansion-contraction slope. The friction slope is computed using the Manning's equation. Detailed description is available in Chandra and Perumal(1985-86).

EFFECT OF CHANNEL CHARACTERISTICS

The effect of channel characteristics on flood wave propagation is studied in the perspective of loop or hysteresis of rating curves. The following hypothetical study is carried out using the dam break flood of the Vagai dam explained below:

The Vaigai dam built across River Vaigai is located near Madurai in the State of Tamil Nadu, India. It is an earthen dam of 25.10 m height with masonry spillway. The reservoir behind the dam has the capacity of 303.38 million cubic metre at the top of the dam. The reservoir is in operation since 1955. In total, 41 cross-sections of the downstream river reach were surveyed for the dam break analysis by National Weather Service's DAMBRK Model. The usual guide lines laid down by the DAMBRK manual(1981) were followed for computing the dam break flood which is shown in Fig. 1. The routing of this dam break flood through the downstream reach length of 72.5 km is carried out using the NWS DAMBRK Model . The top width and slope variations at different locations are shown in Figs. 2a and 2b, respectively. The computed η values at different downstream locations are shown in Fig. 2c. It is visible that the η values show a rising trend at the locations where the channel slope (Fig. 2b) decreases along the channel, for example, in the reach 10-12 km and 24-26 km. The η values also attain relatively high values at the locations where the channel passes through expansion/contraction, viz. at 46.5 km and at 45.5 km. The η values attain relatively low values at the locations where channel slope changes from milder to steeper, viz. at 9 km, 20 km, and 34 km. The inference is that the channel characteristics play a significant role in deciding the kind of wave occurring at a location in the channel, the waves are more dynamic at the locations where greater energy loss takes place than they will be in otherwise situation. Figs. 3 and 4 show respectively the variation of attenuation and phase difference with the non-dimensional hysteresis.

From the above analysis it is evident that a systematic study is required for looking at the impact of varying channel characteristics on the flood wave propagation. For this, the routing of the above Vaigai dam break flood through a hypothetical reach of 72 km is carried out for various channel geometries. The assumed channel reach characteristics are shown in Table 2 and the computed non-dimensional hystereses at

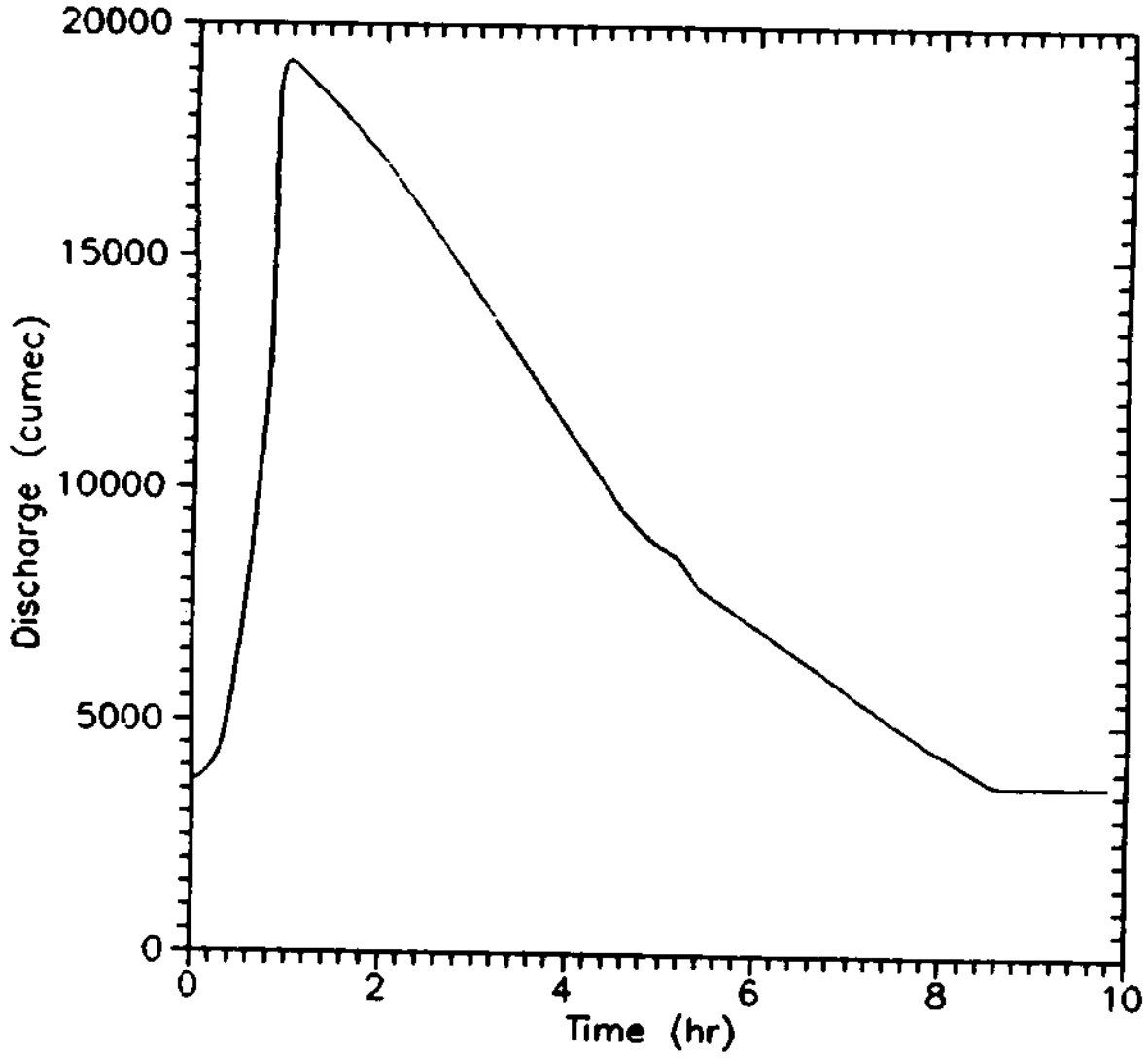

Fig. 1. Vaigai dam break. flood hydrograph.

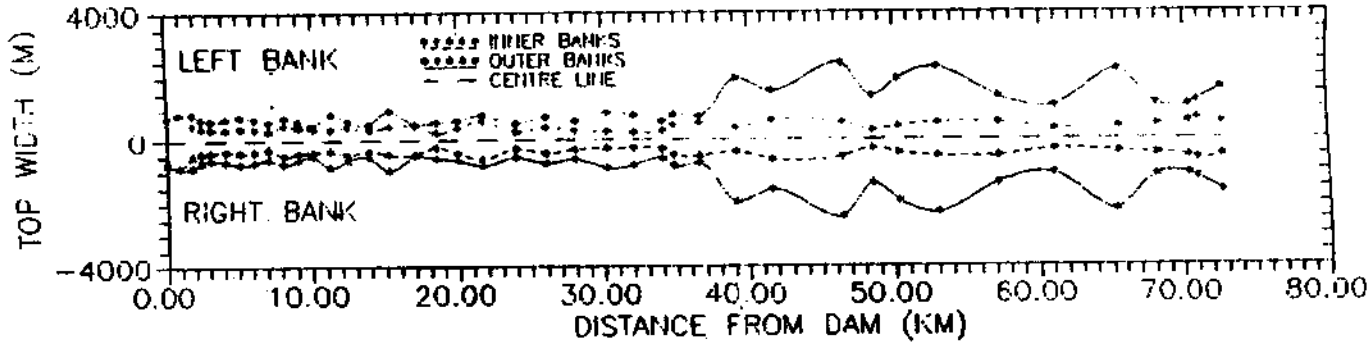

(a) Plan view of the river valley (with available cross-sections represented by *)

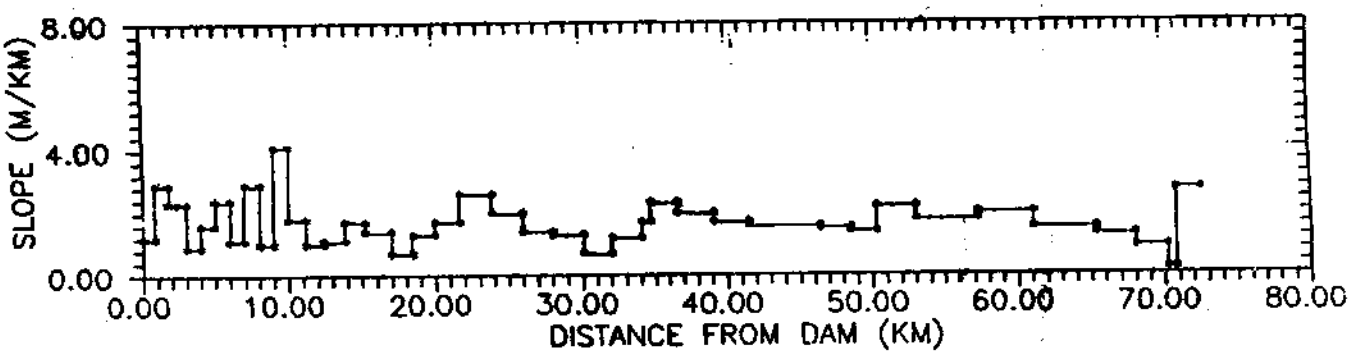

(b) Bed slope variation along the river valley.

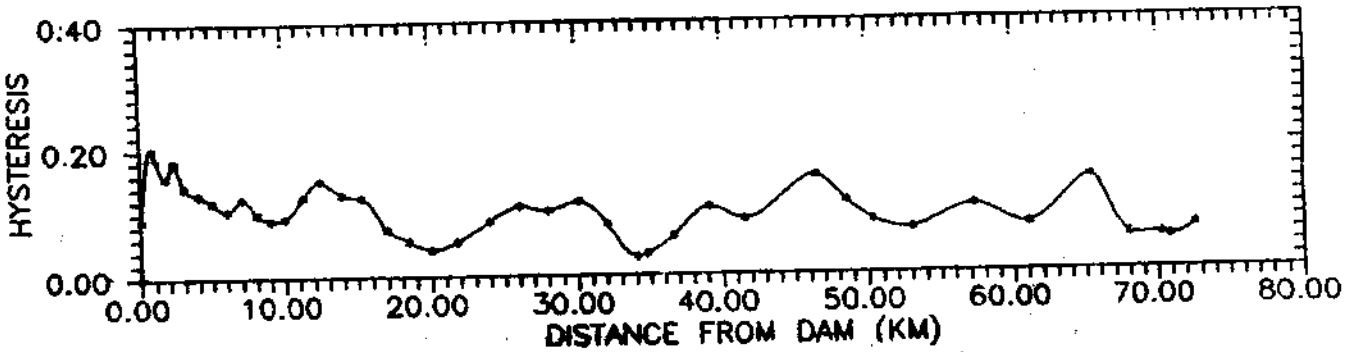

(c) Hysteresis variation along the river valley. Zero km corresponds to the dam site.

Fig. 2. Vaigai dam failure study.

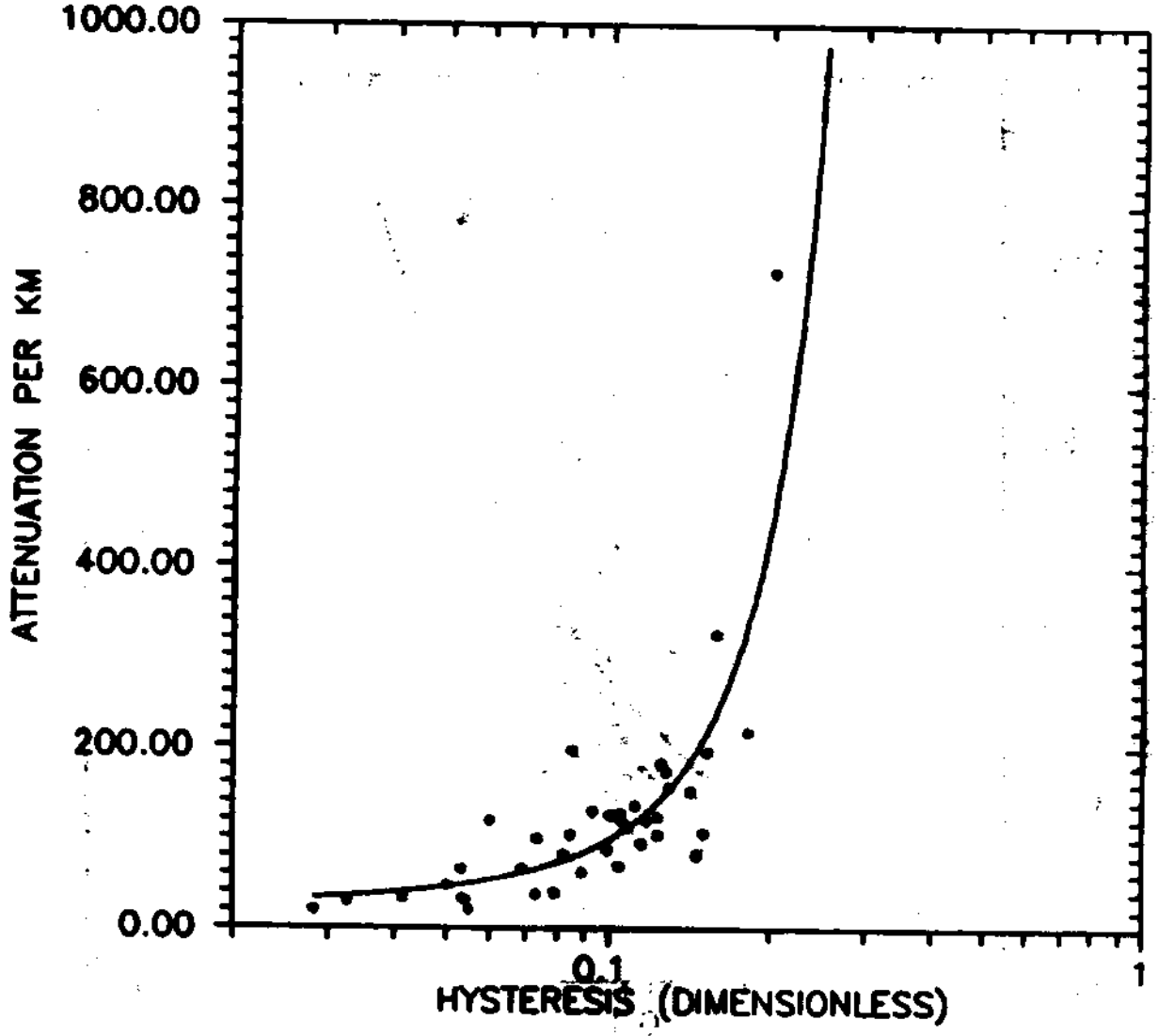

FIG. 3. DIMENSIONLESS HYSTERESIS VS. ATTENUATION PER KM

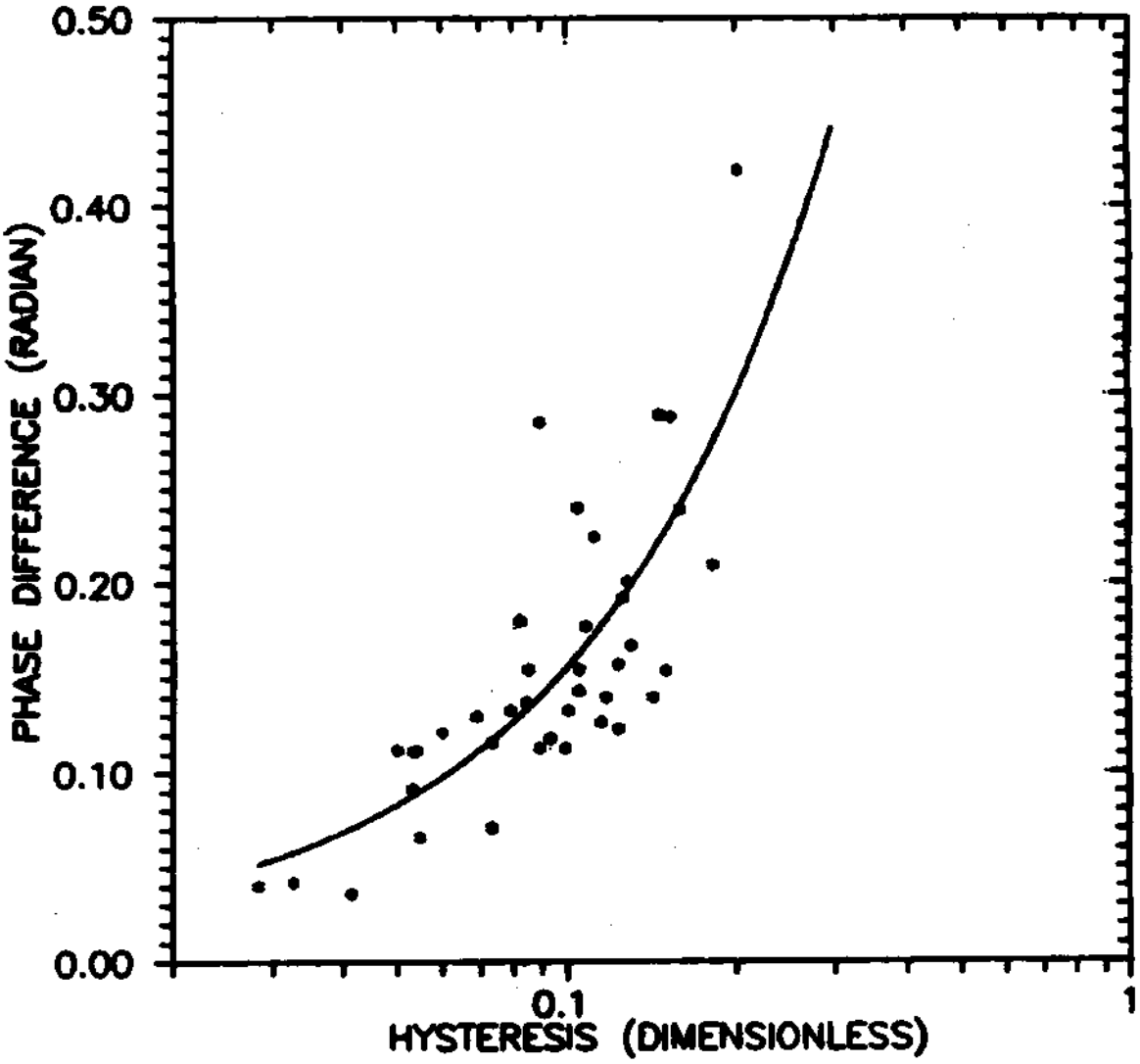

FIG. 4. DIMENSIONLESS HYSTERESIS VS. PHASE DIFFERENCE (RADIAN)

TABLE 2. DESCRIPTION OF TEST RUNS

Run No.	Channel Characteristics						
	Shape	Expansion/ contraction	Exp/cont. coeff.	S_o (m/km)	Manning's roughness 'n'	Flood Plain	Inactive Storage
1	Rectangular	No	0.0	1.6883	0.040	No	No
2	Triangular	No	0.0	1.6883	0.040	No	No
3	Rectangular	Contraction	0.1	1.6883	0.040	No	No
4	Rectangular	Expansion	0.5	1.6883	0.040	No	No
5	Rectangular	Contraction-expansion	0.1-0.5	1.6883	0.040	No	No
6	Rectangular	Expansion-contraction	0.5-0.1	1.6883	0.040	No	No
7	Rectangular	No	0.0	1.6883	0.030	No	No
8	Rectangular	No	0.0	1.6883	0.050	No	No
9	Rectangular	No	0.0	1.6883	0.040	FP1	No
10	Rectangular	No	0.0	1.6883	0.040	FP2	No
11	Rectangular	No	0.0	1.6883	0.040	No	Yes
12	Rectangular	No	0.0	0.1000	0.040	No	No

TABLE 3. SUMMARY OF COMPUTED HYSTERESIS(η) FOR THE TEST RUNS

Run No	Location (km)				
	0	18	36	54	72
1	0.0511580	0.0635881	0.0849514	0.0615482	0.0583086
2	0.0730143	0.0597734	0.0699015	0.0590134	0.0524883
3	0.0430336	0.0591421	0.0579653	0.0546608	0.0571232
4	0.0500994	0.0664043	0.0571384	0.0549793	0.0564528
5	0.0457497	0.0859299	0.0480928	0.0571022	0.0546656
6	0.0412369	0.0554132	0.0668402	0.0587740	0.0696592
7	0.0423517	0.0471487	0.0557070	0.0484810	0.0690041
8	0.0721264	0.0777063	0.0595322	0.0689917	0.0646191
9	0.1094599	0.1644611	0.0910501	0.1517448	0.0836020
10	0.2517080	0.0566349	0.0609694	0.0549345	0.0522299
11	0.0821629	0.0750866	0.0681973	0.0649891	0.0621147
12	0.4773908	0.4399872	0.3806581	0.3469501	0.2732353

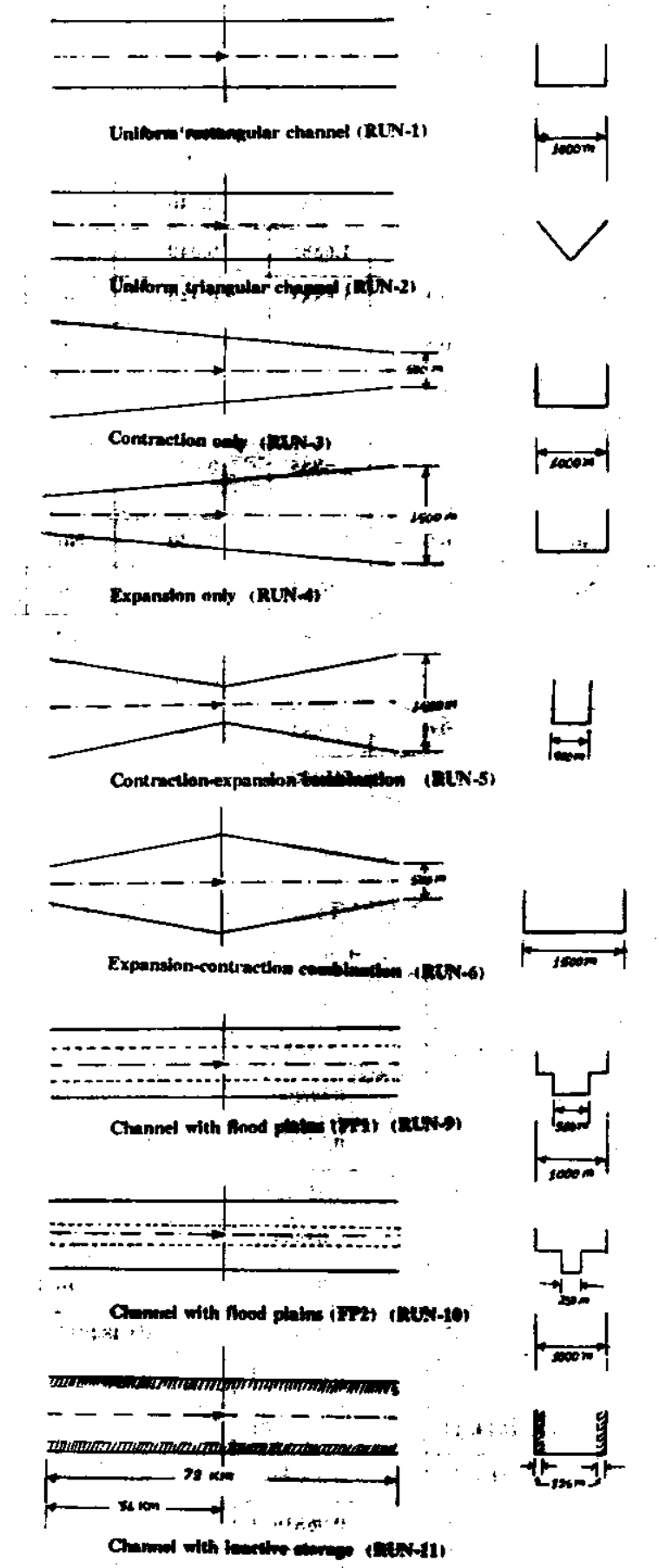

Fig. 5. Assumed channel characteristics for various test runs.

different downstream locations in Table 3. It is again to emphasize that the greater hysteresis value represents greater size of the loop in rating curve at a site under consideration and the smaller hysteresis value the smaller size of the loop. The larger the hysteresis, the more dynamic is the flood wave and vice versa.

The effect of various channel characteristics (Fig. 5 and Table 2) on the flood wave propagation is studied with respect to RUN-1 described in Table 2; RUN-1 corresponds to uniform rectangular channel. For this, the hysteresis value of a run at a location in the channel reach is divided by the hysteresis value that corresponds to RUN-1 at the same location. This ratio is shown on the ordinates of Figs. 6 and 7. If the ratio is greater than 1.0 at a location, the hysteresis value at that location is larger than that due to RUN-1 or indirectly, the flood wave is more dynamic at that location than that due to RUN-1 at the same location. If the ratio is less than 1.0, the flood wave is less dynamic at that location than that due to RUN-1 at the same location. It is worth mentioning that the η values have been computed at five locations, 0, 18, 36, 54 and 72 km. only and a linear variation in η between two consecutive locations is assumed. The surface area of the channel at the highest elevation, supplied to the NWS DAMBRK model as input, is kept same in all the cases.

Effect of Channel Shape

It is apparent from Fig. 6 that the η-ratio (ordinate) decreases sharply in the reach 0-18 km and then mildly in the reach 18-36 km. It increases mildly in the reach 36-54 km and again decreases. It shows that in the reaches 0-18 km and 18-36 km, the attenuation per km is greater in the triangular shaped channel than in the rectangular channel or the triangular shaped channel causes greater energy loss to the flood wave than the rectangular one in wave propagation. This phenomenon can be explained as follows. The constriction posed by the triangular channel causes the dam break flood to attain greater depth of flow in the reach 0-18 km., and thereby, increases the wetted perimeter. The greater the wetted perimeter, the greater will be the friction loss, and consequently, the greater will be the η value, and thus, the greater will be the attenuation per km.

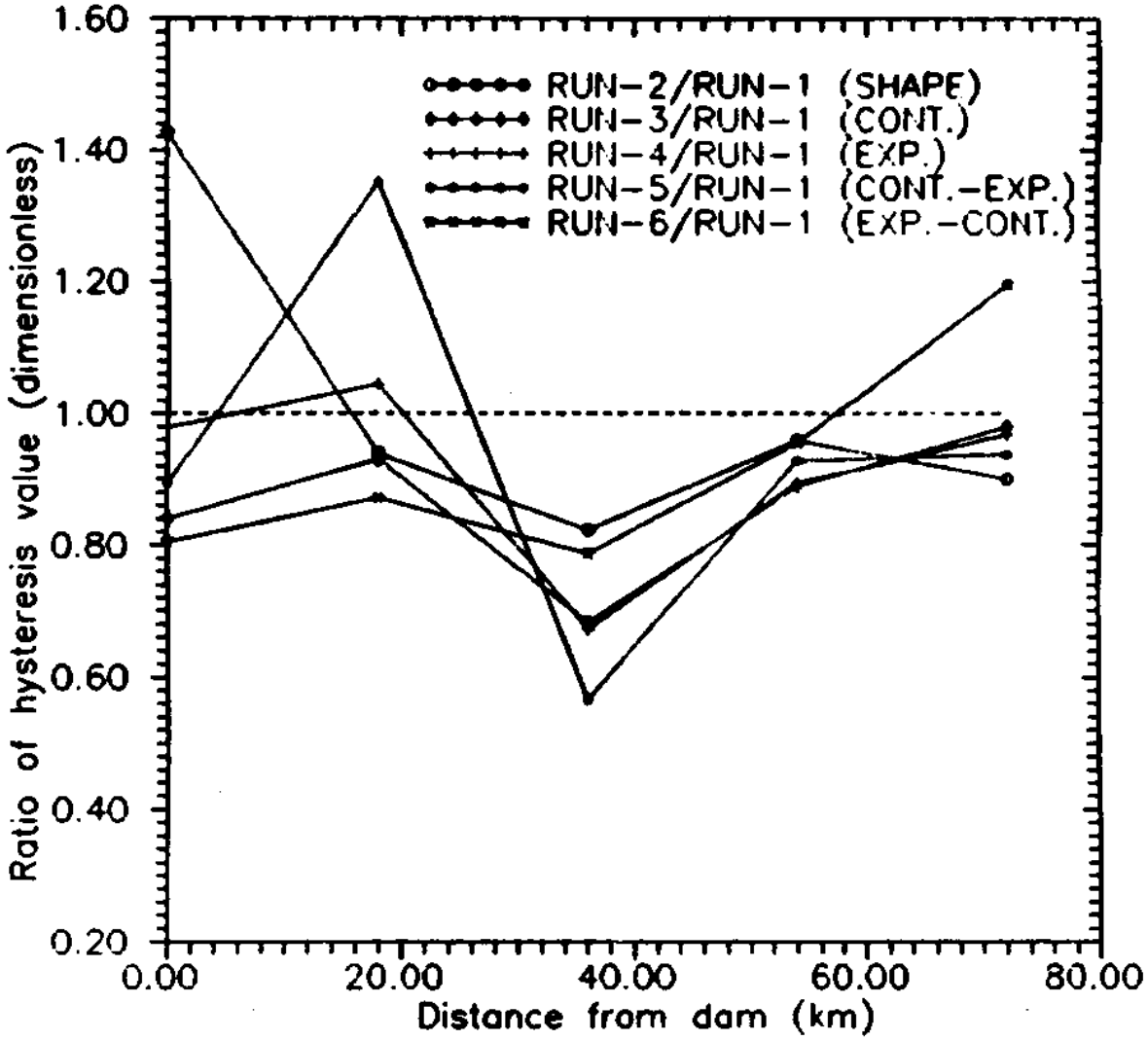

Fig. 6. Impacts of channel shape, contraction, expansion, expansion–contraction combination, and contraction–expansion combination.

The greater attenuation caused in the reach 0-18 km alleviates the intensity of the flood peak discharge greater than that in rectangular shaped channel. In the remaining reach 18-72 km, the η values being less than 1.0 indicate that the attenuation per km in the rectangular channel is greater than that in the triangular shaped channel. It is consistent with the analytical work of Rutschmann and Hager(1996) dealing with the analysis of diffusion waves. The contrasting behaviour in the reach 0-18 km might be attributed to the shape of the flood wave deviating much from the sinusoidal wave form.

Effect of Contraction Only

Fig. 6 shows η-ratio values less than 1.00 at all the locations inferring these being greater in uniform channel than these in laterally constricted channel. This can be explained as follows. The lateral constriction of the channel reach posed by continuously contracting the channel downstream (Fig. 5) causes the wave to attain greater velocity at a location than that in the uniform channel. The greater the average velocity of flow at a section, the greater will be the wave celerity of the flow since the latter depends on the former. The greater the wave celerity of flow, the lesser will be the attenuation (Price (1973,1985); and Mishra and Seth (1994, 1996)). Indirectly, the η values in the laterally constricted channel will be lower than those in the uniform channel.

Effect of Expansion Only

As evident from Fig. 6, the η-ratio values in the case of lateral expansion is greater than those in lateral contraction, and greater than 1.00 in the reach 6-20 km. Therefore, expansion poses greater energy loss than the contraction. It might also be attributed to the recommended and used higher coefficient values of the expansion coefficient (Table 2). Trends of η-ratio variation along the channel is the same as of contraction.

Effect of Contraction-Expansion Combination

In the reach 2-23 km (Fig. 6), the η-ratio values are greater than 1.00, and in the remaining reach, these are less than 1.00. The trend of η-ratio variation with the

distance is the same as of contraction or expansion but it is more pronounced in the contraction part than in the expansion part of the channel reach. It is indicative that the greatest attenuation occurs not at the point of minimum top width (at 36 km), but at a location upstream.

Effect of Expansion-Contraction Combination

The expansion followed by contraction shows (Fig. 6) the same trends in η-ratio variation along the channel as in contraction-expansion combination. But it is more pronounced in the contraction part than in the expansion part of the channel reach. Furthermore, indicated is that the maximum attenuation occurs not at the point of minimum top width (at 36 km),but at some other location downstream.

Effect of Roughness

The effect of channel roughness (Manning's n) is shown in Fig. 7. The greater the Manning's n, the greater is the η-value. When n=0.03 (less than that in RUN-1), the energy loss is less than that due to RUN-1. When n=0.05 (greater than that in RUN-1), the energy loss is greater than that due to RUN-1. The same is reflected through the Fig. 7 except in the reaches 26-30 km and 64-72 km. In the former case, η-ratio is less than 1.00, and in the latter, it is greater than 1.00. It is consistent with the conclusion of Cunge et al.(1980). They, however, attributed it to the increase in unsteadiness of flow rather than the energy loss.

Effect of Flood Plain

The effect of flood plains on the flood wave propagation is examined with respect to two cases shown in Fig. 5. These cases, FP1 and FP2, are differentiated by the lateral length of the flood plains. That with smaller flood plains pertains to FP1 and the larger to FP2. The total top width above a certain depth is, however, the same (=1000 m) in both the cases. Fig. 7 shows the values of the η-ratio at all locations are greater than 1.0 indicating greater hysteresis or attenuation or lesser celerity at all the locations than those in a rectangular channel (due to RUN-1) at the corresponding locations. In the

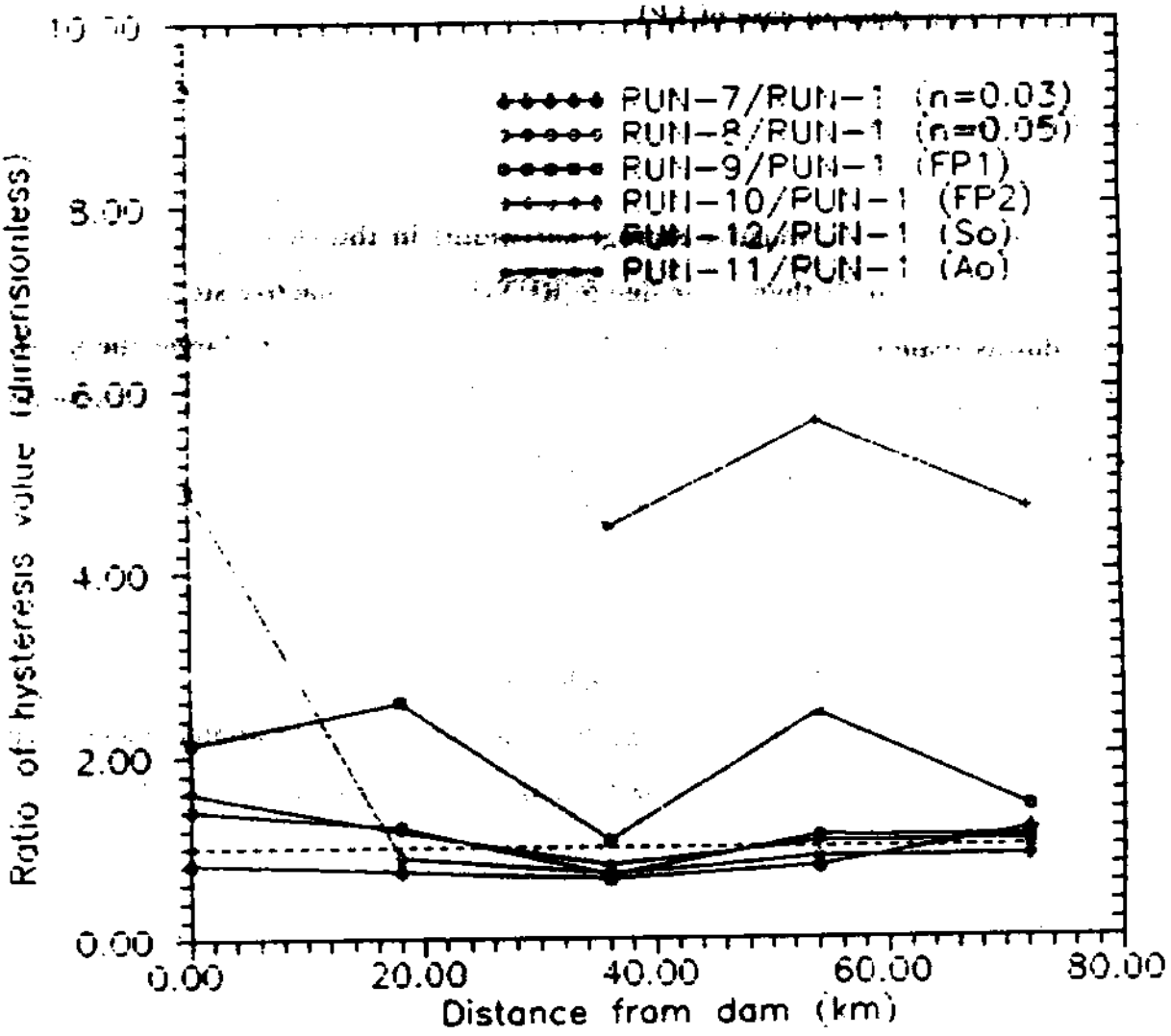

Fig. 7. Figure showing impacts of bed slope (So), Manning's roughness (n), flood plain (FP1 & FP2) and inactive storage (Ao).

reach 0-12 km, the FP2 shows greater η-ratio than the FP1. After approximately 18 km these values are less than 1.00. This can be explained as follows. The constriction posed to the channel at the lower depths causes the flood to attain greater depth of flow. Secondly, it causes an increase in the wetted perimeter of the flow resulting in an increase in the energy loss. Greater energy loss in the reach 0-12 km in case of FP2 makes the flood wave subside greater than that in case of FP1. The greater reduction in the flood magnitude makes the flood wave less dynamic, and in turn, shows smaller η-ratio values than those in case of FP1.

Effect of Inactive Storage

The introduction of inactive storage (or width) in the channel (Fig. 5) causes larger hystereses (Table 3) than those due to RUN-1 without inactive storage at all the locations downstream except in the reach 26-50 km. Alternatively, the larger the η-ratio (Fig. 7), the lesser will be the celerities and the greater the attenuation than those due to rectangular channel without inactive storage.

Effect of Bed Slope

The reduced bed slope, by approximately ten times (Table 2), has the most significant impact on the quantified hysteresis values at all the locations (Table 3 and Fig. 7). It causes the greatest energy loss than any other characteristics of the channel.

ANALYTICAL DERIVATIONS

Assuming that h (Eq. 2) and q (Eq. 3) follow the following cosine wave form:

$$h = H\cos(\sigma x - \beta t) \tag{6}$$

$$q = Q\cos(\sigma x - \beta t - \phi) \tag{7}$$

where, $\sigma = 2\pi/L$; L(=cT) is the wave length; $\beta = 2\pi/T$; H and Q are the non-dimensional amplitudes of h- and q-waves, respectively; and x is the space coordinate. Putting Eq. 6 and 7 in Eq. 1 leads to the following:

$$\eta = \pi QH \sin\phi \tag{8}$$

Since both h and q range 0-1, each H and Q will be equal to 1/2. This leads Eq. 8 to be recast as

$$\eta = \frac{\pi}{4}\sin\phi \tag{9}$$

For $\phi=0$ (kinematic wave situation) or π (gravity wave situation), $\eta=0$; η attains maximum value of $\pi/4$ when $\phi=\pi/2$ (dynamic wave situation). If h-wave precedes q-wave, η will be negative. Taking the logarithm of Eq. 7, differentiating with respect to x, and then making non-dimensional using L lead to:

$$\delta_k = 2\pi\tan\phi \tag{10}$$

Here, subscript 'k' refers to kinematic wave situation. Eq. 10 can also be derived from the relation developed by Menendez and Norscini(1982) for kinematic wave situation. Positive δ shows attenuation, and negative the amplification. If h-wave precedes q-wave, δ will be negative. Using Eq. 9 and 10, a relation for kinematic wave situation can be derived as below:

$$\frac{8\eta}{\sin\phi} = \frac{\delta_k}{\tan\phi} = 2\pi \tag{11}$$

Verification of η-ϕ Relationship

Based on the results of numerical experimentations by Mishra and Seth(1996) and Jain et al.(1996), Mishra et al.(1997) postulated a relation, $\eta=0.6366\ \phi$, which is close to the analytical derivation, $\eta=0.7854\ \phi$ (Eq. 10: as $\phi\rightarrow 0$, sin $\phi\rightarrow\phi$). The analytical and numerical results are also compared in Fig. 8. Evidently, the η values computed using Eq. 1 and those using analytical relation (Eq. 9) are, in general, close to the line of perfect agreement. Deviation of some data points is, however, attributed to the numerical computational errors.

Development of Energy Index for Input Flood Wave

Fig. 9 shows a relation between η and δ . Three distinct trends are apparent showing dependence of attenuation on an unknown third parameter. In an attempt to relate it with the energy index of input flood wave (Table 4), it is found that given the ϕ, the flood waves with greater input energy attenuates more than those with lesser input energy. Here, input energy index is defined as the product of the discharge- and depth-amplitude divided by the square of time period (second last column of Table 4). On the whole, the results infer that δ is a function of η which, in turn, is the result of ϕ.

TABLE 4. CHARACTERISTICS OF INPUT FLOOD WAVES

Dam	Location	Q_{max} (cusec)	Q_{min} (cusec)	H_{max} (ft)	H_{min} (ft)	T (hr)	Energy Index*	Reference
Teton	Idaho,USA	1640429	13000	96.09	11.90	5.80	0.3143	Mishra and Seth (1994, 1996)
Machhu II	Gujarat,India	1936970	278920	59.35	34.50	7.20	0.0613	Mishra and Seth (1994, 1996)
Bargi	Madhya Pradesh,India	4316030	1480206	174.54	103.30	34.00	0.0135	Mishra et al. (1997) and Jain et al.(1996)

Note: * Energy Index= $(Q_{max}-Q_{min})\,(H_{max}-H_{min})\,/\,T^2$; here, T is in second.

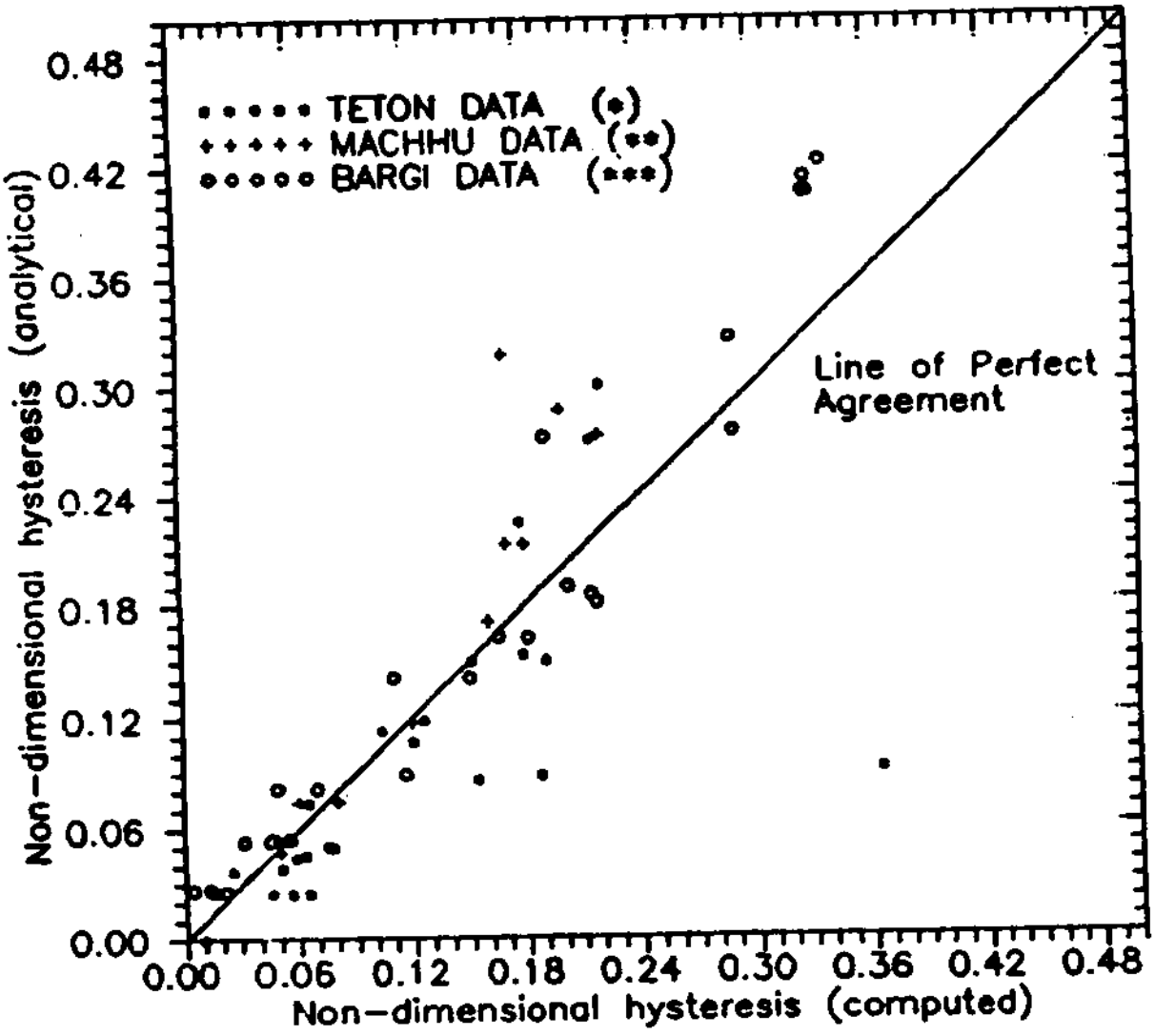

Fig. 8. Comparison of computed non-dimensional hystereses (Eq. 1) and those derived analytically (Eq. 9); data (*) & (**) used by Mishra & Seth(1996); and (***) by Mishra et al. (in press)

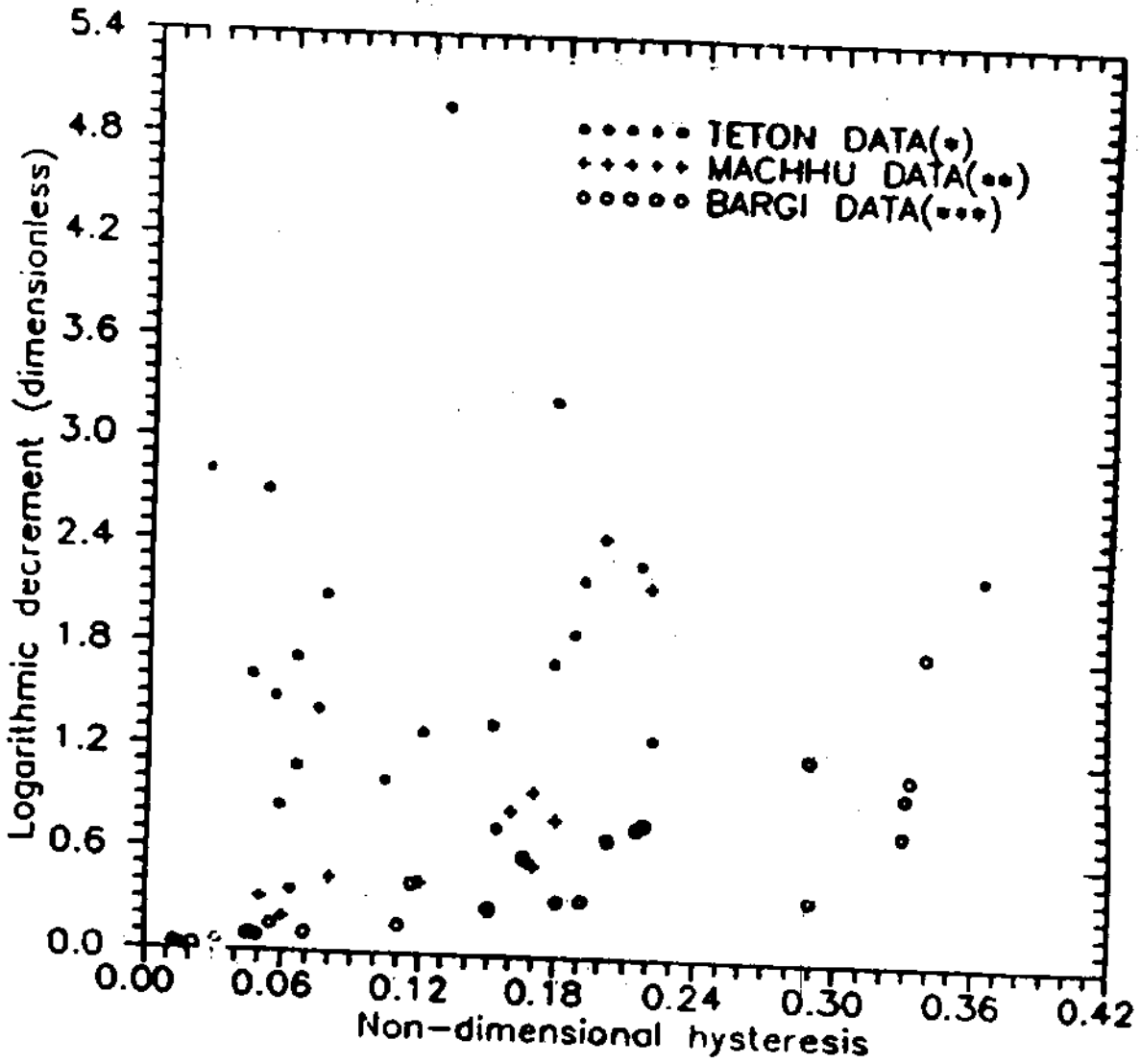

Fig. 9 Relation between non-dimensional hysteresis and logarithmic decrement (dimensionless). Data(*) & (**) used by Mishra & Seth(1996); and (***) used by Mishra et al. (in press)

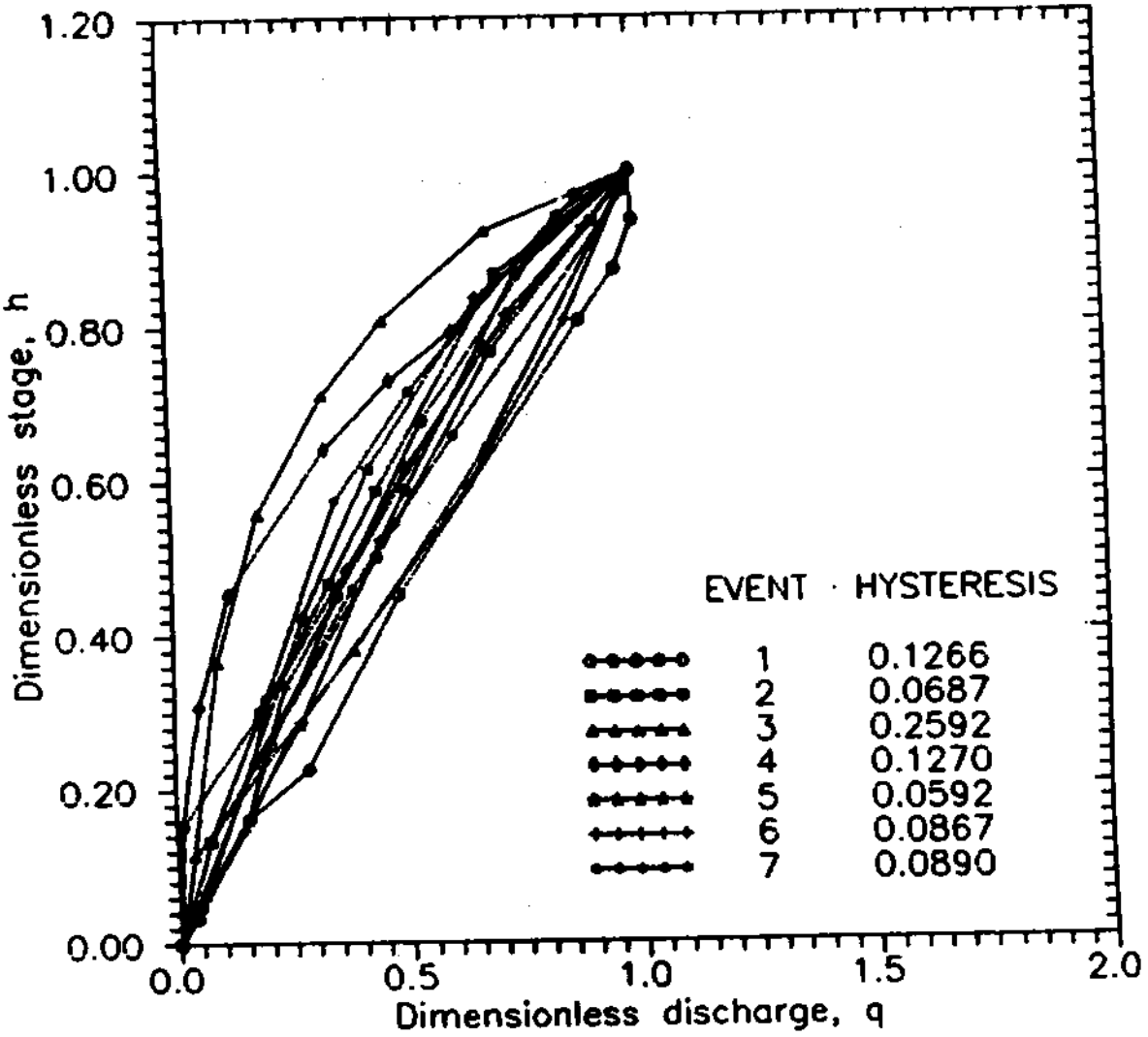

Fig. 10. Observed loop rating curves (dimensionless)

Application to Observed Flood Events

Mistry et al.(1984) observed loop rating curves shown in Fig. 10 in dimensionless form. The details of these flood events are given in Table 5. The analysis of these flood events (Table 6) shows that the flood events fall under the category of either dynamic wave (DYW) or diffusion wave (DW) (Table 1). The computed ϕ using Eq. 9 are in close agreement with those computed using the observed data, $\phi_{obs.}$, and so do the time periods,T. The relative errors in ϕ range between +8.80% and -3.24% and in T, these vary from -8.06% to +3.31%. In general, the results not only supports the validity of Eq. 9 but also lend an alternative way for computing time base of the flood hydrographs which might be of use in base flow separation studies.

TABLE 5. DETAILS OF FLOOD EVENTS OBSERVED ON THE RIVERS IN GUJARAT (INDIA)

Event	River	Station	District	Period	Q_{max} (cumec)	Q_{min} (cumec)	H_{max} (m)	H_{min} (m)	t_{pb} (hr)	t_{pQ} (hr)
1	Mazar	Kathlal	Kheda	Aug. 10-13, 1981	270.00	19.24	3.50	0.40	16.938	15.114
2	Mindhola	Bardoli	Surat	Aug. 9-11, 1982	182.99	35.67	2.10	0.60	23.648	22.671
3	Karjan	Thawa	Bharuch	Jun. 25-27, 1980	336.22	13.02	2.85	0.25	25.081	22.476
4	Panam	Sant Road	Panchmahal	Aug. 16-17, 1981	3935.88	135.00	4.50	0.60	8.860	7.818
5	Meshwo	Mithajina-Mavada	Sabarkanthi	Aug. 17-18, 1981	291.98	30.00	2.10	0.28	10.423	9.772
6	Ambika	Umai	Valsad	Jul., 18-21, 1983	300.35	25.93	1.55	0.20	23.453	21.889
7	Watrak	Mahemdabad	Kheda	Jul., 24-26, 1982	329.48	45.00	2.20	0.44	32.899	31.922

Data Source: Mistry et al. (1984)

TABLE 6. APPLICATION RESULTS OF OBSERVED FLOOD EVENTS

Event	η	Wave type	ϕ (obs.) (radian)	ϕ (comp.) (radian)	Error in ϕ (%)	T (obs.) (hr.)	T (comp.) (hr.)	Error in T (%)
1	0.1266	DYW	0.1488	0.1619	+8.80	77.00	70.79	- 8.06
2	0.0687	DW	0.0877	0.0875	- 0.23	70.00	70.16	+0.23
3	0.2592	DYW	0.3274	0.3363	+2.72	50.00	48.67	- 2.66
4	0.1270	DYW	0.1625	0.1624	- 0.06	40.30	40.31	+0.03
5	0.0592	DW	0.0693	0.0754	+8.80	59.00	54.25	- 8.05
6	0.0867	DW	0.1143	0.1106	- 3.24	86.00	88.85	+3.31
7	0.0890	DW	0.1077	0.1136	+5.48	57.00	54.04	- 5.26

NOTATIONS: DW stands for diffusion wave, and DYW for dynamic wave.

CONCLUSION

The results of the present study have revealed that the bed slope, flood plains, channel shape, expansion-contraction combination, expansion-contraction combination, inactive storage, Manning's roughness, expansion, and contraction impacts the flood wave propagation in the order of their significance in respect of generally increasing the quantified hysteresis. The larger the hysteresis, the larger will be the phase difference and attenuation and lesser will be the celerity of the flood wave. The developed analytical relation (Eq. 9) between hysteresis and phase difference has been verified using available numerically derived data and seven observed flood events. The definite relationship between them shows that the former also describes attenuation. The existence of a definite relation between the above attenuation parameters has also been described through a unique relation which is valid in the realm of kinematic wave.

REFERENCES

Chandra S. and M. Perumal(1985-86),'Data requirement and data preparation for DAMBRK programme,' Technical Note, National Institute of Hydrology, Roorkee-247 667, UP, India.

Cunge, J.A., F.M. Holly Jr., and A. Verwey(1980),'Practical aspects of computational river hydraulics,'Pitman Advanced Publishing Program, Boston.

French, R.H.(1985),'Open channel hydraulics,'McGraw-Hill Book Co.,Inc.,New York, NY,551

Henderson, F.M.(1966),'Open channel flow,'Macmillan,New York,USA.

Jain, M.K., S.K. Mishra and S.M. Seth(1996),'Hysteresis criteria for the applicability of CPC and CPMC methods of flood routing,' Proc. Int. Conf. on Disasters and Mitigation, Anna University, Madras (India), Jan. 19-22.

Menendez, A.N. and R. Norscini(1982),'Spectrum of shallow water waves: An analysis,'J. Hydr. Div., ASCE, 108(HY1), 75-94.

Menendez, A.N. and R. Norscini(1983),discussion on 'Nature of flood wave attenuation in open channel flow,'J. Hydr. Div., ASCE, 109(5),pp.786-789.

Mishra, S.K., S.M. Seth(1994),'Effect of downstream boundary conditions on dam break flood wave propagation characteristics,' Tech. Rep., National Institute of Hydrology, Roorkee (India).

Mishra, S.K., M.K. Jain and S.M. Seth(1997),'Characterization of flood waves by rating curves,' J. Nordic Hydrology, Vol. 28(1), 1997.

Mishra. S.K., S. Sah, N. Sharma, and S.M. Seth(1996),'Defining flood wave propagation characteristics using hysteresis of rating curves,' HYDRO96, Dec. 11-13, IIT, Kanpur, India.

Mistry, J.F., D.M. Naik, R.Y. Pathak(1984),'Estimation of flood discharge by loop rating curves,' 51st Ann. Res. & Dev. Sess., Central Board of Irrigation & Power, Vadodara, Gujarat (India), Jan. 2-5, 57-70.

National Weather Service (NWS) (1981),'The NWS dam-break flood forecasting model: Users manual,' Davis, California, USA.

Ponce, V.M.(1989),'Engineering Hydrology: Principles and Practices,'Prentice Hall, Englewood Cliffs, New Jersey.

Ponce V.M. and D.B. Simons(1977),'Shallow wave propagation in open channel flow,'J. Hydr. Div.,ASCE,103(HY12),1461-1476.

Price, R.K.(1973),'Flood routing methods in British rivers,'Proc. Instn. Civil Engrs. (London), Part 2, Vol. 57, 913-930, paper 7674.

Price,R.K.(1985),'Flood routing,'Ch. 4 of Developments in Hydraulic Engineering, E.J.P. Novak, Elsevier Applied Science.

Rutschmann, P. and W.H. Hager(1996),'Diffusion of flood waves,' J. Hydrology, Elsevier, Vol. 178(1996),pp. 19-32.

DIRECTOR	**DR. S.M. SETH**
DIVISIONAL HEAD	**SH. R.D. SINGH**
SCIENTIST	**SH. S.K. MISHRA**
TECHNICAL STAFF	**SH. R.K. NEMA**
STENO	**SH. T.P. PANICKER**